Structural and adhesional properties of thin MoO_3 films prepared by laser coating

Structural and adhesional properties of thin MoO_3 films prepared by laser coating

Mihail Mihalev[1,5], Chavdar Hardalov[2], Christo Christov[2], Michail Michailov[3], Bogdan Ranguelov[3]and Harald Leiste[4]

[1]Faculty of Mechanical Engineering, Technical University of Sofia,
8 Kliment Ohridski Blvd., 1000 Sofia, Bulgaria
[2]Department of Applied Physics, Technical University of Sofia,
8 Kliment Ohridski Blvd., 1000 Sofia, Bulgaria
[3]Institute of Physical Chemistry, Bulgarian Academy of Sciences,
Akad. G. Bonchev Str., Building 11, 1113 Sofia, Bulgaria
[4]Insitute of Applied Materials – Applied Materials Physics,
Karlsruhe Institute of Technology, Karlsruhe, Germany

E-mail: mmihalev@tu-sofia.bg

Abstract. Laser marking plays an important role in numerous technological applications because of its flexibility, fastness and versatility. The present study deals with the structural and adhesional properties of thin MO_3 layers on stainless steel substrates prepared by a specific modification of the laser coating technology known as “laser bonding”. This approach consists in the local laser sintering of an initially deposited proper powder material, which forms under laser irradiation a layer with a definite graphical and topological design. The coatings, prepared of only MoO_3 powder irradiated by a CO_2 laser beam, are well bonded to the substrate and exhibit diffusive light reflection. Through applying a variety of methods for surface structural analysis, as micro-indentation, XRD, micro-Raman and SEM, this study also provides detailed information about the coatings’ chemical bonding and composition. Our results reveal a good adhesion to the steel due to the formation of an amorphous interface between the MoO_3 and the substrate. This amorphous interface arises from a “quenching” process of the molten MoO_3 acting both as an oxidant and flux. Depending on the laser beam’s intensity, energy and scanning velocity, we also observed recrystallization in specific areas of the coatings. The present study contributes to the better understanding of the adhesion, wear-resistance and hardness of MoO_3 coatings obtained by laser bonding.

1. Introduction

A new versatile technology [1], which is similar to the laser cladding – the so called “laser bonding”, has been known since 1997. A complex powder mixture, consisting of pigments, oxides, glazes and silicates is irradiated by a laser source, thus heating the powder. As a result, a stable coating with different optical, mechanical and structural properties is formed on the steel surface. According to the patent cited, the chemical bond is realized through iron silicate.

[5] To whom any correspondence should be addressed.

We have implemented a modification of the technology of laser bonding, based on a laser treatment of MoO_3 powder on stainless steel. This material was chosen as a typical transition metal oxide. It is well known that MoO_3 is a very aggressive oxidant in its liquid phase [2, 3], acting as a flux ([3] and references therein) as well. It produces an iron molybdate interface on the substrate [4, 5, 6]. Moreover, the colour of the powder is changed to dark violet/black, so that no additional pigments are necessary, which is aim of the direct laser marking.

2. Experimental setup and procedure for laser coating

The equipment used for laser coating was a 50-W cw sealed CO_2 laser. The laser beam was steered by a standard XY fly optics moving system (with a high scanning velocity of up to 30 m/min) to a 50-mm focusing ZnSe lens, thus forming a focal spot of approximately 200 μm diameter on the sample.

For the substrate, grade 304 stainless steel was chosen. It was pre-coated with 99.9 % α-orthorhombic MoO_3 (CAS Number 1313 – 27 – 5) using a spray gun [7].

Two types of samples were prepared: 1) a static laser beam was used (forming a nearly circular structure, see figure 1 left and middle), when the laser beam does not move over the sample, called by us "point samples" and 2) the laser beam scanned the sample at a given sweep rate (see figure 2 right), called by us as "raster-scanned samples". The sweep rate and the raster step were controlled by a CNC unit. More details were presented in [8, 9].

In the case of point samples, CO_2 laser pulses of different durations were applied: 10 ms, 100 ms, 1000 ms. The pulses of 10 ms and 100 ms produced similar SEM images, thus the image with 10-ms pulse duration was omitted.

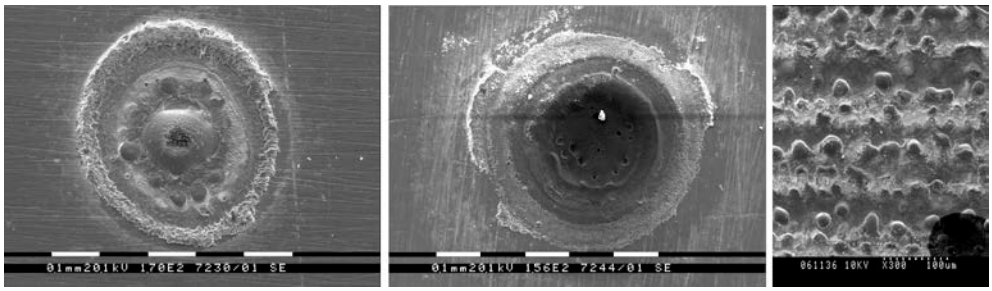

Figure 1. SEM of typical spots at 100 ms (left) and 1000 ms (middle) exposure time, and (right) SEM image of a typical raster-scanned laser bonded coating.

3. Experimental results and discussion

3.1. Mechanical properties

3.1.1. Vickers hardness. The Vickers hardness test was conducted using a CSEM Revetest scratch tester with a Vickers shaped indenter.

The hardness test of the substrate and coating, averaged over 3 measurements at 3 different points, yielded values of 302 HV0.05 and 251 HV0.06, respectively. However, it must be noted that these data should be considered as indicative only, because 1) the substrate is not undeformable, and 2) in a hardness measurement, the coating thickness must be at least one order of magnitude larger then the indentation depth, which was not the case in our samples. Nevertheless, it can be assumed that the coating possessed hardness comparable with that of the steel.

Figure 2. Micrograph of scratch trace: top: 50× magnification; bottom: 500× magnification – at the beginning, middle and end of test (from left to right).

3.1.2. Adhesion. To the best of our knowledge, no methods exist that provide an unambiguous quantitative evaluation of the adhesion. All methods describe more or less phenomenologically the process of coating failure.

One standard method is the ramp scratch test [10]. A CSEM Revetest scratch tester was used again.

In the ramp test, the load was varied from 0 to 100 N at a rate of 10 N/min, while the sample was moved at 5.7 mm/min.

The micrographs of the scratch trace at 50× and 500× microscope magnification show no material failures, even at 100 N (figure 2). The material was dragged by the indenter, building a groove of increasing depth and width. This fact is indicative of strong plastic deformations in the material due to the well-known layered structure of MoO_3 [11], which implies usages as surfaces that are locally tribologically changed. No critical load was found at which coating failure could be observed. Moreover, at the end of the test, when the maximal load of 100 N was reached, the indenter scraped the substrate, but traces of the coating on the substrate could still be noticed. These facts support unambiguously the assumption for an excellent coating-to-substrate adhesion.

3.2. R*aman spectroscopy*

3.2.1. Point sample. Micro-Raman spectroscopy was performed by a HORIBA LabRAM HR spectrometer with an incorporated He-Ne laser (wavelength 633 nm).

Figure 3a) presents micro-Raman spectra acquired from three point samples irradiated by the CO_2 laser at different exposure times – 10 ms, 100 ms and 1000 ms.

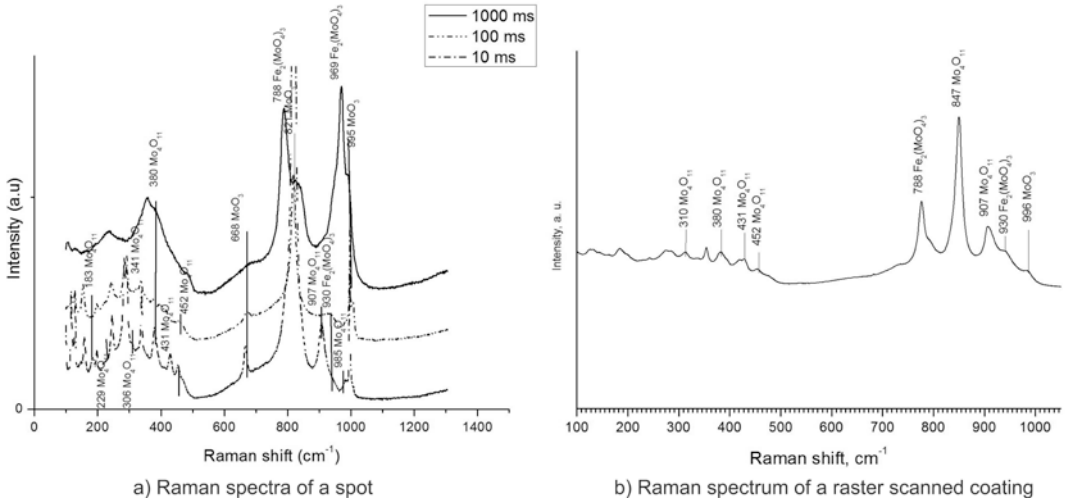

Figure 3. Raman scattering spectra of a point sample (left) and a raster-scanned sample (right).

In all spectra (10 ms, 100 ms and 1000 ms) the most typical Raman lines of orthorhombic MoO_3 at 668 cm^{-1}, 822 cm^{-1} and 995 cm^{-1} [12] are seen.

In the spectrum of the sample with the shortest exposure time of 10 ms, the following lines are seen in addition to the MoO_3 lines: 183 cm^{-1}, 229 cm^{-1}, 306 cm^{-1}, 341 cm^{-1}, 380 cm^{-1}, 431 cm^{-1}, 452 cm^{-1}, 907 cm^{-1} and 985 cm^{-1}, which can be associated with a more complex orthorhombic molybdenum oxide, namely, Mo_4O_{11} [13].

When the exposure time was raised to 100 ms, a new line, that of iron molybdate $Fe_2(MoO_4)_3$, appeared at 930 cm^{-1} [14] in addition to the lines of Mo_4O_{11} and MoO_3.

The longest exposure time resulted in broadening and in lowering the intensity of Mo_4O_{11} and MoO_3 lines, while the lines of $Fe_2(MoO_4)_3$ 788 cm^{-1}, 930 cm^{-1} and 969 cm^{-1} [14] became narrower and with higher intensities. No MoO_2 Raman lines were detected.

In the case of the very short CO_2 laser exposure time of 10 ms, the presence of MoO_3 lines can be explained by the existence of initial material that has not been melted. No $Fe_2(MoO_4)_3$ molybdate lines are observed. This exposure time is too short for formation of substantial amount of iron molybdate for a detectable Raman scattering. We believe that molybdate serves as an interface between the steel and the coating. The presence of the most typical lines of Mo_4O_{11} can be explained with the exposure time leading to a rapid non-equilibrium re-crystallization process.

Under the conditions of a longer exposure time (100 ms), the amount of $Fe_2(MoO_4)_3$ increases, resulting in the appearance of the new line at 930 cm^{-1}.

At 1000 ms, the intensities of the $Fe_2(MoO_4)_3$ lines are much higher the those of the lines of all other oxides. We believe that substantial amounts of MoO_3 and Mo_4O_{11} are vaporized at the high temperature in the zone affected by the laser light (as evidenced by the concave meniscus in the point sample), so that the He-Ne laser beam can reach the $Fe_2(MoO_4)_3$ interface. At the shorter exposure times, the oxide scale absorbs the He-Ne beam and the Raman signal is much lower.

It must be noted that, at the centre of all point samples (10, 100, 1000 ms), an amorphous phase is seen (wide lines in their bases, ending with sharp peaks, which is an indication of Raman scattering on different non-collective and collective bonds, respectively), due to the extremely high temperature and time gradients and the lack of re-crystallization as a result of the Gaussian intensity distribution of the CO_2 laser beam.

3.2.2. Raster-scanned samples. Figure 3b) presents a typical spectrum of a coating produced by raster-scanning the CO_2 laser beam. Depending on the raster-scanning step (distance between individual scanning lines), the CO_2 laser beam passes through a given point several times, leading to multiple re-crystallization of the molten bead. Generally, lines of all above-mentioned compounds, MoO_3, Mo_4O_{11}, $Fe_2(MoO_4)_3$, are observed in the spectrum with various intensities, due to the convolution of concurrent Raman peaks from both crystallites and amorphous phases during the laser processing.

3.3. Analysis of the XRD spectra

Unlike Raman spectroscopy, XRD is less sensitive to absorption by the coating due the high photon energy; thus, the signal originates from all depths of the coating, including the interface and the substrate.

The measurements were performed on a Seifert PTS300 spectrometer with a Cu-Kα line (λ = 1,5405 nm). A typical XRD pattern of a raster-scanned sample is presented in figure 4.

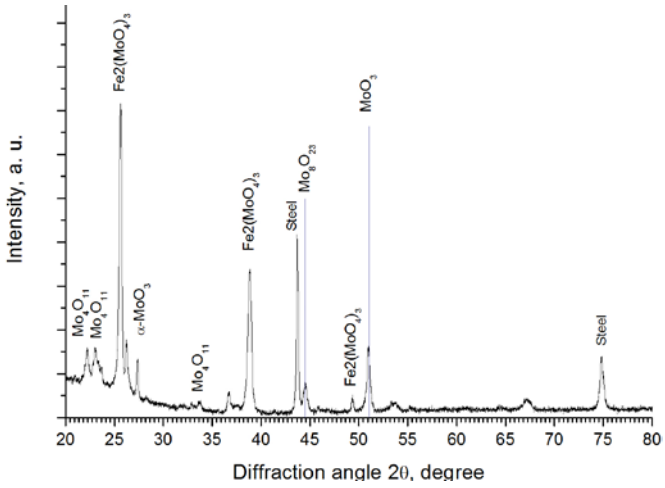

Figure 4. XRD pattern of a raster-scanned coating.

In accordance with the JPCPDS (card numbers 5-508, 5-503, 5-452, 5-337, 89-2367, 89-2368) data bases, the presence of the following compounds was established: MoO_3, Mo_4O_{11}, $Fe_2(MoO_4)_3$, as well as steel [15] (figure 4), which is in agreement with the Raman scattering data for the same sample. Reference to the JPCPDS data bases for MoO_2 and $Fe(MoO_4)$ did not reveal the presence of these compounds.

The experiments on Vickers hardness showed that the coatings possessed hardness against normal penetration comparable to the metal hardness. Moreover, no material failure was observed during the scratch test, which can be explained by the typical layered structure of MoO_3 [11].

The Raman spectroscopy and XRD measurements showed the formation of additional compounds, namely, Mo_4O_{11} and $Fe_2(MoO_4)_3$ from the initial powder, as well as the presence of some initial un-

melted MoO_3. This can be explained by the occurrence of complex non-equilibrium physical and thermo-chemical processes, induced by i) enormous temperature gradients, ii) fast temperature rise time and iii) fast quenching processes in the melt.

The heating of the initial powder leads to a very high temperature in the laser-affected zone (in the range of 1500 – 2000 °C, as the FEM model in [9] predicts). In its molten phase, MoO_3 acts as an aggressive oxidant, as well as effective flux ([16] and references therein). As a result, an interface consisting of $Fe_2(MoO_4)_3$ is formed. $Fe_2(MoO_4)_3$ is chemically bonded to the substrate, as all our tests confirm. The presence of MoO_3 and Mo_4O_{11} and the absence of MoO_2 is, in our opinion, in accordance with the catalytic and autocatalytic properties of MoO_3 [17]. At the longest CO_2 laser exposure time, a well expressed erosion of the substrate surface was observed (see figure 1, middle), which also supports the assumption of an intensive oxidation.

4. Conclusions

The formation of the coating is a result of complex phenomena with a number of processes acting simultaneously. The very high temperature and the fast temperature rise time initiate the chemical transformation of MoO_3 to the intermediate oxide Mo_4O_{11}, which is a stable phase. The formation of the amorphous phase is a result of the fast quenching of the molten powder. Due to the properties of MoO_3, acting both as an oxidant and a flux, an interface of $Fe_2(MoO_4)_3$ appears. The inter-diffusion between $Fe_2(MoO_4)_3$, MoO_3 and intermediate oxides seems to be responsible for the good adhesion of the coating to the substrate. Taking into account: i) the good adhesion, ii) the absence of material failures at scratch and iii) surface roughness leading to diffusive reflection, this technology, in our opinion, can be used for direct laser marking meeting the respective requirements [18], as well as for improving the wear-resistance of stainless steels.

To the best of our knowledge, all existing technologies for laser marking that use laser bonding are based on multi-component liquid or dry mixtures, known in the industry as “laser marking inks”. This paper contributes to the better understanding of the physical and thermo-chemical processes in such type of technologies.

The study of high-temperature physical and chemical transient processes in the millisecond range requires sophisticated “in-situ” equipment and will be the subject of future works.

Acknowledgments

The support of KNMF/ANKA, KIT, Germany and of Prof. Miroslav Abrashev, University of Sofia, are gratefully acknowledged.

References

[1] Harrison and Wollcott P 1997 *US Patent 6075223*
[2] Brenner S S 1955 Catastrophic oxidation of some molybdenum alloys *J. Electrochem. Soc.* **102**/1 16-21
[3] de Van J H 1961 Catastrophic oxidation of high-temperature alloys *Oak Ridge National Laboratory* **10**
[4] Berdzenishvili I G 2012 Functional corrosion-resistant enamel coatings and their adherence strength *Proc. Int. Congress Adv. Appl. Phys. Mater. Sci.* (Antalya Turkey 2011) pp 178-80
[5] *Fundamentals of Adhesion* 1991 ed L. H. Lee (Springer Verlag)
[6] Fick D, Layne C, Gnizak D and Evele H 2001 Iron oxide interfacial reactions as related to enamel bonding *Proc. 63rd Porcelain Enamel Institute Technical Forum: Ceramic Engin. Sci.* vol 22 issue 5
[7] Mihalev M, Hardalov Ch, Chirstov C G and Leiste H 2013 Microstructural characterization of thin laser bonded coatings based on transitional metal oxides powder *Proc. 23d Nat. Symp. Metrology and Metrology Assurance* (Sept. 2013 Sozopol Bulgaria) pp 219-25
[8] https://ecad.tu-sofia.bg/e-publ/files/1102_69_1.pdf
[9] Christov C G, Mihalev M S and Hardalov Ch M 2010 Characterization of thin MoO_3 layers

obtained by laser bonding *J. Technol.* (Assumption University Bangkok Thailand) **14**/1 1-10
[10] Taube K 1994 Mechanische charakterisierung an duennen schichten 1994 *J. für Oberflächentechnik* **11** 83-7
[11] Rao M C, Ravindranadh K, Kasturi A and Shekhawat M S. 2013 Structural stoihometry and phase transitions of MoO_3 thin films for solid state microbatteries *Res. J. Recent Sci.* **2**/4 67-73
[12] Dieterle M and Mestl G 2002 Raman spectroscopy of molybdenum oxides: Structural characterization of oxygen defects in MoO_{3-x} by DR UV/VIS Raman spectroscopy and X-ray diffraction *Phys. Chem. Chem. Phys.* **4** 812-21
[13] Dieterle M and Mestl G 2002 Raman spectroscopy of molybdenum oxides: Resonance Raman spectroscopic characterization of the molybdenum oxides Mo_4O_{11} and MoO_2 *Phys. Chem. Chem. Phys.* **4** 822-6
[14] Xu Q, Jia G, Zhang J, Feng Z and Li C 2008 Surface phase composition of iron molybdate catalysts studied by UV Raman spectroscopy *J. Phys. Chem.* C **112** 9387–93
[15] *pcpdfwin software for XRD diffraction patterns*
[16] Young D J 2008 *High Temperature Oxidation and Corrosion of Metals* (Elsevier Linacre House UK)
[17] Thijs F, Piet M and Paul G J 1979 Monolayer- and crystal-type MoO_3 catalysts: Their catalytic properties in relation to their surface structures. *J. Colloid and Interface Sci.* **70**/1 97-104
[18] NASA technical standard *NASA-STD-6002A* Sept. 2002 NASA USA